

# Local S100A8 Levels Correlate With Recurrence of Experimental Autoimmune Uveitis and Promote Pathogenic T Cell Activity

Juan Yun,<sup>1</sup> Tong Xiao,<sup>1</sup> Lei Zhou,<sup>2-4</sup> Roger W. Beuerman,<sup>2-4</sup> Juanjuan Li,<sup>1,5</sup> Yuan Zhao,<sup>6</sup> Amir Hadayer,<sup>1</sup> Xiaomin Zhang,<sup>7</sup> Deming Sun,<sup>8</sup> Henry J. Kaplan,<sup>1</sup> and Hui Shao<sup>1</sup>

<sup>1</sup>Department of Ophthalmology and Visual Sciences, Kentucky Lions Eye Center, University of Louisville, Louisville, Kentucky, United States

<sup>2</sup>Singapore Eye Research Institute, Singapore

<sup>3</sup>Department of Ophthalmology, Yong Loo Lin School of Medicine, National University of Singapore, Singapore

<sup>4</sup>Ophthalmology and Visual Sciences Academic Clinical Research Program, Duke-NUS Medical School, Singapore

<sup>5</sup>Department of Ophthalmology, The 2nd People's Hospital of Yunnan Province, Kunming, Yunnan Province, China

<sup>6</sup>Department of Pharmaceutical Sciences, Sullivan University College of Pharmacy, Louisville, Kentucky, United States

<sup>7</sup>Department of Uveitis & Ocular Immunology, Tianjin Medical University Eye Hospital, Eye Institute & School of Optometry and Ophthalmology, Tianjin, China

<sup>8</sup>Doheny Eye Institute, Department of Ophthalmology, David Geffen School of Medicine, UCLA, Los Angeles, California, United States

Correspondence: Hui Shao, Kentucky Lions Eye Center, Department of Ophthalmology and Vision Sciences, University of Louisville, 301 E. Muhammad Ali Boulevard, Louisville, KY 40202, USA; h0shao01@louisville.edu.

Submitted: October 10, 2017

Accepted: January 31, 2018

Citation: Yun J, Xiao T, Zhou L, et al. Local S100A8 levels correlate with recurrence of experimental autoimmune uveitis and promote pathogenic T cell activity. *Invest Ophthalmol Vis Sci.* 2018;59:1332–1342. <https://doi.org/10.1167/iovs.17-23127>

**PURPOSE.** To investigate the role of damage-associated molecular patterns (DAMPs) in recurrent experimental autoimmune uveitis (EAU).

**METHODS.** Recurrent EAU was induced in Lewis rats by interphotoreceptor retinoid-binding protein (IRBP) R16-peptide specific T cells (tEAU). Aqueous humor and serum samples were kinetically collected and DAMPs examined by quantitative proteomics, Western blot analysis, and ELISA. tEAU rats were treated with S100 inhibitor paquinimod followed by disease evaluation. The functions of T effector cells and T regulatory cells (Tregs) were compared between treated and nontreated groups. The expression of costimulatory molecules on antigen-presenting cells was examined by flow cytometry.

**RESULTS.** S100A8, but not high mobility group box 1 (HMGB1), in the eye was found to be correlated with intraocular inflammatory episodes. Administration of paquinimod significantly protected tEAU rats from recurrence. Treated tEAU rats had fewer R16-specific Th1 and Th17 cells, but increased numbers of Tregs. R16-specific T cells from treated tEAU rats into naïve recipients prevented induction of tEAU by R16-specific T cells from nontreated tEAU rats. Moreover, APCs from treated tEAU rats expressed higher levels of a negative costimulatory molecule, CD200R, and lower levels of CD80, CD86, and MHC class II molecules compared to APCs from nontreated tEAU rats. An opposite pattern of expression of these molecules was observed on APCs incubated in vitro with recombinant S100A8.

**CONCLUSIONS.** Our data demonstrate a link between local expression of DAMPs and autoimmune responses, and suggest that complete S100A8/A9 blockade may be a new therapeutic target in recurrent autoimmune uveitis.

**Keywords:** recurrent autoimmune uveitis, immune regulation, autoreactive T cells, damage-associated molecular patterns, S1008/9, HMGB1

Autoimmune (idiopathic) uveitis in humans can be acute, chronic, or recurrent, in the last of which the intraocular inflammation shows relapses and remissions that vary in frequencies and timing. The complications caused by repeated inflammation and damage inside the eye, as well as by long-term drug treatment, lead to visual impairment, which accounts for approximately 10% of legal blindness in the Western world.<sup>1</sup> In studies using animal models of experimental autoimmune uveitis (EAU), with characteristics of the human disease, it has been found that the disease is associated with activation of autoreactive T cells.<sup>2</sup> Adoptive transfer of activated T cells reactive with retinal antigens, such as interphotoreceptor retinoid-binding protein

(IRBP), induces chronic uveitis in mice<sup>3</sup> and recurrent uveitis in Lewis rats.<sup>4,5</sup> In the recurrent form of tEAU, the first episode of intraocular inflammation starts at day 4 and is followed by varying numbers of remissions. Similar to the clinical signs often seen in the human disease,<sup>4</sup> neither the duration of a single disease peak nor the interval between episodes is predictable; in addition, the right and left eyes of a single recipient often show a different rhythm of relapse. This tEAU model provides us with a useful tool for studying the regulation of pathogenic effector T cells in vivo during the course of the disease.

A number of mechanisms may contribute to the remitting-relapsing character of the disease. Inter- and intramolecular



spreading that shifts the immunoreactivity of T effector cells has been demonstrated in equine spontaneous recurrent uveitis<sup>6</sup> and recurrent autoimmune anterior uveitis in Lewis rats immunized with myelin basic protein.<sup>7</sup> We have previously reported that CD4<sup>+</sup>CD25<sup>+</sup> regulatory T cells (Tregs) make a significant contribution to controlling an ongoing inflammatory response in the eye and that dysregulation and malfunction of local Tregs is an important factor in disease recurrence, persistence, and progression.<sup>8</sup> In addition, we have found that ligation of exogenous or endogenous pathogen/damage-associated molecular patterns (PAMPs/DAMPs) to pathogen recognition receptors on intraocular parenchymal cells, such as astroglial cells, can reduce the threshold at which autoreactive T cells are activated in the eye.<sup>9–11</sup> Stimulation of astroglial cells with PAMPs/DAMPs increases the expression of MHC and costimulatory molecules and induces production of IL-6, IL-12, and IL-23, leading to the activation of Th1 and Th17 IRBP-specific T cells.<sup>10</sup> One of the major endogenous DAMPs, high-mobility group box 1 (HMGB1), is immediately released as a consequence of the interaction of activated uveitogenic T cells with parenchymal cells.<sup>12</sup> HMGB1 promotes CXCL12 release from parenchymal cells, and the combination of HMGB1 and CXCL12 enhances leukocyte migration.<sup>13</sup> The recruitment of leukocytes, including T cells and monocytes, as well as the release of ocular antigens from damaged ocular tissues, might promote uveitogenic T cell activation, since HMGB1 antagonists or blockade of binding of CXCL12 to its receptor CXCR4 reduce ocular inflammation and suppress uveitogenic T cell proliferation and Th1 and Th17 cytokine production.<sup>12,14</sup> These findings indicate that the innate immune response, including PAMP/DAMP release, is involved in sustaining T cell-mediated adaptive autoimmune uveitis. However, the correlation of HMGB1 with the recurrence of intraocular inflammation is unknown.

S100A8, another important DMAP member is a small-sized 10-kDa molecule and preferentially exists as a heterodimer or heterotetramer with S100A9, known as calprotectin (S100A8/A9).<sup>15</sup> These molecules are highly expressed on bone marrow-derived myeloid cells, specifically neutrophils and monocytes, and on endothelial cells.<sup>15</sup> During the early phase of the immune response, infiltrating myeloid cells release S100A8/9 at local sites of inflammation.<sup>16–19</sup> Serum levels of this complex have been used as a very early and sensitive biomarker for local inflammatory activity<sup>15</sup> and are also highly increased during wound-healing processes, tumorigenesis, and autoimmune disorders.<sup>20</sup> Released extracellular S100A8/A9 exerts several paracrine and autocrine effects and stimulates monocytes and macrophages by binding to RAGE, toll-like receptor (TLR) 4, and other receptors required for the activation of MAPK- and NF- $\kappa$ B signaling-dependent mechanisms,<sup>15</sup> thus leading to increased production of proinflammatory molecules and cytokines.<sup>21</sup> S100A8/A9 also stimulates autoreactive T cells.<sup>22</sup>

In the tEAU model induced by transfer of R16-specific T cells in rats, the disease is triggered by pathogenic effector T cells without contamination by microbial components used in direct antigen injection models (aEAU). Using tEAU model, we examined whether there were associations between S100A8/9 and HMGB1 levels in the AqH and blood and each episode of intraocular inflammation, focusing on the effects of S100A8/9 on the regulation of pathogenic effector T cells and Tregs that might account for the recurrent and remission character of the disease.

## MATERIALS AND METHODS

### Animals and Reagents

Pathogen-free female Lewis rats (5- to 6-week-old) were purchased from Envigo (Indianapolis, IN, USA), and housed

and maintained at the animal facilities of the University of Louisville (Louisville, KY, USA). All animal studies conformed to the ARVO Statement for the Use of Animals in Ophthalmic and Vision Research. The protocol (#17095) was approved by the Institutional Animal Care and Use Committee of the University of Louisville and institutional guidelines regarding animal experimentation were followed. The bovine IRBP peptide R16 (residues 1177–1191, ADGSSWEGVGVVDPV) was synthesized by Sigma-Aldrich Corp. (St. Louis, MO, USA).

### Preparation of R16-Specific T Cells

R16-specific T cells were isolated from R16-immunized Lewis rats using previously described methods.<sup>4,5</sup> T cells were isolated from the draining lymph nodes and spleen at 12 days postimmunization (p.i.) by passage through a nylon wool column. The cells ( $1 \times 10^7$ ) were then stimulated for 2 days with 20  $\mu$ g/mL R16 in 2 mL complete medium (CM; RPMI 1640 [Mediatech, Manassas, VA, USA] supplemented with 10% fetal calf serum [FCS; Hyclone, Logan, UT, USA],  $5 \times 10^{-5}$  M 2-mercaptoethanol, and 100  $\mu$ g/mL penicillin/streptomycin) in a six-well plate (Costar, Cambridge, MA, USA) in the presence of  $1 \times 10^7$  irradiated syngeneic spleen cells as APCs, then activated lymphoblasts were isolated by gradient centrifugation in Percoll Plus (GE Healthcare Life Sciences, Marlborough, MA, USA) and cultured in RPMI 1640 medium supplemented with 15% IL-2-containing medium (supernatant from Con A-stimulated rat spleen cells).

### Animal Model of tEAU in Lewis Rat and Clinical Evaluation

tEAU was induced by adoptive transfer of activated R16-specific T cells prepared as above into naive Lewis rats ( $3 \times 10^6$ /rat).<sup>4,5</sup> The injected rats were examined daily for clinical signs of uveitis by slit-lamp biomicroscopy and the intensity of uveitis was scored blind on an arbitrary scale of 0 to 4, as described previously,<sup>4</sup> with 0 as no disease, 1 as engorged blood vessels in the iris and an abnormal pupil configuration, 2 as a hazy anterior chamber, 3 as a moderately opaque anterior chamber, with the pupil still visible, and 4 as an opaque anterior chamber, obscured pupil, and, frequently, proptosis.

### Pathological Examination

Inflammation of the eye was confirmed by histopathology. Whole eyes were collected, immersed for 1 hour in 4% phosphate-buffered glutaraldehyde, and transferred to 10% phosphate-buffered formaldehyde until processed. The fixed and dehydrated tissue was embedded in methacrylate, and 5- $\mu$ m sections were cut through the pupillary-optic nerve plane and stained with hematoxylin and eosin. Presence or absence of disease was evaluated blind by examining six sections cut at different levels for each eye. Severity of EAU was scored on a scale of 0 (no disease) to 4 (maximum disease) in half-point increments, as described previously.<sup>4</sup>

### Collection of AqH and Serum

AqH (20  $\mu$ L/rat) was collected from both eyes by anterior chamber puncture using a 30-gauge needle under a surgical microscope and stored immediately in a  $-80^\circ\text{C}$  freezer until use for quantitative proteomics using isobaric tags for relative and absolute quantitation (iTRAQ) and Western blot.

Blood was collected from the vena cava and left 30 minutes at room temperature to clot, then was centrifuged at 9300g for 10 minutes and the serum removed and stored immediately in a  $-80^\circ\text{C}$  freezer until use for ELISA.

### Measurement of HMGB1 and S100A8 Levels in AqH by Western Blot Analysis

AqH in one R16-T cell injected rat (5  $\mu$ L) was mixed with 5  $\mu$ L 2  $\times$  Laemmli reducing sample buffer and heated at 95° for 5 minutes, then was run on SDS polyacrylamide gels. Western blotting was performed on nitrocellulose membranes (Bio-Rad, Hercules, CA, USA) as described previously<sup>10</sup> using anti-S100A8 Ab (Santa Cruz, Dallas, TX, USA) and anti-HMGB1 Ab (Abcam, Cambridge, MA, USA). Rat spleen was used as a positive control for S100A8 and HMGB1.

### Measurement of HMGB1 and S100A8 Levels in Serum by ELISA

Samples of serum (5  $\mu$ L) were diluted 1:10 in the buffer included in the kit and added to wells precoated with HMGB1 (Abcam) or S100A8 (R&D Systems, Minneapolis, MN, USA) capture Abs, then HMGB1 or S100A8 levels were measured following the manufacturer's instructions.

### Treatment of tEAU With an S100 Inhibitor

Naïve Lewis rats were treated with the Q compound paquinimod (ABR-215757; a gift from Active Biotech AB, Lund, Sweden), a compound that blocks binding of S100A9.<sup>23,24</sup> The compound (PA) was used at an oral dosage of approximately 25 mg/kg/day, starting 1 day before T cell transfer and continuing throughout the experiment.<sup>25</sup> To achieve this dose in a rat weighing approximately 200 g and drinking approximately 20 mL water/day, 0.25 mg/mL PA was added to the drinking water, the water bottles being replaced every other day. Plain drinking water was supplied to the controls. There were no evident side effects against rats including the weight changes in these treated rats.<sup>24,26</sup>

### Assays for R16-Specific T Cell Proliferation and Cytokine Production

Nylon wool-enriched T cells prepared from pooled spleen on the indicated days after transfer of R16-specific T cells were seeded at  $4 \times 10^5$  cells/well in 96-well plates and cultured at 37°C for 60 hours in a total volume of 200  $\mu$ L CM alone or CM containing the indicated concentrations of R16 in the presence of irradiated syngeneic spleen APCs ( $1 \times 10^5$ ), and BrdU incorporation during the last 8 hours was assessed using BrdU assay kits (Roche, Indianapolis, IN, USA). The proliferative response was expressed as the mean OD  $\pm$  SD for triplicate samples or the proliferative stimulus index calculated as the ratio of the mean OD measured in the presence of the Ag to that in the absence of Ag and the experiment was performed three times, with similar results. To measure cytokine production by responder T cells, supernatants were collected after 48 hours of T cell stimulation as above and assayed for IFN- $\gamma$ , IL-17, and IL-10 using ELISA kits (R&D Systems).

### Isolation of Cells From Inflamed Eyes

After perfusion of the anesthetized rat with PBS on the indicated day after transfer of T cells, the eyes were collected and a cell suspension prepared by digestion for 10 minutes at 37°C with collagenase (1 mg/mL) and DNase (100  $\mu$ g/mL) in RPMI 1640, followed by gradient centrifugation on 25% Percoll and subsequent Ficoll separation, then the cells were washed and resuspended in staining buffer (PBS containing 3% FCS and 0.1% sodium azide) for antibody staining.<sup>8,27</sup>

### Immunofluorescence Flow Cytometry

Aliquots of  $5 \times 10^5$  APCs were stained with FITC- or PE-conjugated monoclonal antibodies against rat CD200R, CD80, CD86, or OX6. For staining of Foxp3 Tregs, T cells were incubated for 30 minutes at 4°C with anti-CD4 or isotype control Abs, fixed overnight with 1 mL fixation buffer (Fix and Perm cell permeabilization kit; eBioscience, La Jolla, CA, USA), washed, and incubated for 30 minutes at 4°C with anti-rat-Foxp3 antibody. For intracellular cytokine staining, T cells were pretreated for 4 hours with 50 ng/mL PMA, 1  $\mu$ g/mL ionomycin, and 1  $\mu$ g/mL brefeldin A (all from Sigma-Aldrich Corp.), then were washed, incubated for 30 minutes at 4°C with anti-CD4 or isotype control Abs, fixed, permeabilized overnight with Cytotfix/CytoPerm buffer (eBioscience), and incubated for 30 minutes at 4°C with anti-rat-IFN- $\gamma$  or IL-17 Abs. Data collection and analysis were performed on a FACScaliber flow cytometer using CellQuest software (BD, San Jose, CA, USA). All antibodies used for flow cytometry analysis were purchased from eBioscience.

### Data Analysis

Experiments were performed at least three times. Data analysis for the iTRAQ experiments was performed as described previously,<sup>28</sup> while other statistical analyses were performed using the unpaired Student's *t*-test for two sets of data, 1-way or 2-way ANOVA for three or more means, or the Mann-Whitney *U* test for the pathological score of uveitis. Values determined to be significantly different from those for controls are marked with asterisks in the figures (\**P* < 0.05, \*\**P* < 0.01).

## RESULTS

### Association Between S100A8 Levels in the AqH and Recurrent Uveitis

To explore whether levels of DAMP family molecules correlated with recurrent episodes of EAU, we induced tEAU in Lewis rats by adoptive transfer of R16-specific T cells<sup>4</sup> and collected AqH and sera on days 0 (naïve), 1, 4 (onset), 12 (remission), 19 (second attack), 25 (second remission), and 32 (third attack) for proteomic analysis and Western blot analysis (AqH) and ELISA (serum). We first analyzed protein profiles in the AqH samples by iTRAQ quantitative proteomics. AqH samples from six rats were pooled at each time point and assessed using the Spearman correlation coefficient by analyzing the results for duplicate samples per experiment in two independent experiments. Of the ~200 identified AqH proteins (<1% false discovery rate), 34 were found to correlate with clinical recurrence (Table) and one of these was the DAMP molecule S100A8.

The correlation between S100A8 levels in the AqH with tEAU episodes was confirmed by Western blotting (Fig. 1A). S100A8 was not detected in the naïve eye and on day 1 (before the first episode of intraocular inflammation), but levels were increased during the initial attack (day 4) and during the second and third relapses (days 19 and 32) and reduced during the first and second remissions (days 12 and 25).

We have previously demonstrated that HMGB1, another important DAMP member, is an early and critical mediator in a tEAU model of chronic experimental autoimmune uveitis in mice.<sup>12</sup> As in our previous findings in the eye in mouse tEAU,<sup>12</sup> in the present study, HMGB1 levels were increased on day 1 after T cell transfer and remained high during the entire observation period, even in remission (Fig. 1A).

To determine whether S100A8 and HMGB1 levels in the blood correlated with tEAU score and could be used as

**TABLE.** The Spearman Correlation Coefficient Was Used to Determine if There Was a Nonlinear Relationship Between the Clinical Profile and Protein Relative Expression Level

Proteins	E1	E2
CRP	0.954	0.906
PON1	0.823	0.808
CHI3L1	0.805	0.867
FN1	0.823	0.867
C3	0.823	0.906
FGG	0.823	0.709
SERPINA3K	0.73	0.867
APOE	0.767	0.63
APOA2	0.73	0.906
CFI	0.73	0.709
SERPINA3M	0.711	0.729
AFM	0.767	0.867
HP	0.711	0.591
APCS	0.748	-0.197
ITIH3	0.73	0.906
SERPINA3N	0.711	0.453
F2	0.73	0.591
CP	0.767	0.906
APOA1	0.636	0.906
C9	0.674	0.788
C6	0.617	0.906
HPX	0.655	0.867
FGB	0.636	0.808
FGA	0.636	0.906
C8B	0.636	0.788
APOH	0.543	0.65
LCN2	0.599	0.808
AMBP	0.543	0.788
SERPING1	0.561	0.749
IGH-1A	0.599	0.788
LIFR	0.449	0.906
SERPINA10	0.449	0.473
KNG1	0.356	0.788
S100A8	0.337	0.768

AqH samples were collected on days 0 (naïve), 1 and 4 (onset), 12 (remission), 14 (second attack), 24 (second peak), and 30 (second remission) of tEAU, and analyzed by iTRAQ quantitative proteomics. AqH samples from six eyes were pooled for each time point and assessed using the Spearman correlation coefficient by analyzing duplicate samples in two independent experiments.

biomarkers for attacks and relapses, we measured S100A8 and HMGB1 in serum collected from the same rats tested in Figure 1A and failed to detect any correlation between serum S100A8 and HMGB1 levels and tEAU (data not shown). In addition, we induced tEAU in another three rats (Fig. 1B) and measured their disease score and S100A8 and HMGB1 levels over 34 days and found no correlation between serum S100A8 levels and clinical score, while serum HMGB1 levels showed a similar pattern to those seen in the AqH in Figure 1A.

**Treatment With the S100A9 Inhibitor Paquinimod Reduces Recurrence of Uveitis**

To further determine the importance of S100A8/9 in the recurrence of intraocular inflammation, we treated groups of tEAU rats orally with or without paquinimod (PA), a drug that blocks the binding of S100A9,<sup>23,24</sup> using the protocol described in the Methods section and monitored the clinical score in 6 to 21 rats from each group for 41 days, then examined the pathology (Fig. 2). Other rats from each group were used in further tests described in subsequent sections

(Figs. 3–6). As judged by clinical evaluation, the PA-treated tEAU rats showed reduced inflammation during the first attack and had fewer relapses compared to the controls (Fig. 2A). Pathologic evaluation on day 41 showed infiltrating cells in the vitreous and retinal damage in the control non-PA-treated rats, but not in the PA-treated group (Fig. 2B). We also analyzed eye-infiltrating cells in PA-treated and non-PA-treated rats on day 25 by staining with a panel of antibodies specific for different leukocyte subsets, followed by flow cytometric analysis. As shown in Figure 2C, in the control group, CD4 T cells were dominant during this recurrence, while the PA-treated rats showed a profound reduction in CD4 T cells (42.4% ± 3.1 in the nontreated controls and 10.5% ± 5.9 in the PA-treated group). Percentage of NK cells (control 3.6% + 1.3/treated 1.4% + 1.0) and granulocytes (control 4.6% + 2.2/treated 1.1% + 0.8) were also significantly reduced in the eyes of PA-treated rats. However, percentages of NKT cells (control 3% + 1.9/treated 1.9% ± 1.3) and CD11b cells (control 3.9% ± 1.3/treated 4.4% + 3.0) were not significantly changed between treated and nontreated groups. Since total infiltrating cells were much less in treated eyes than nontreated eyes, the number of cells in each subtype in treated eyes was significantly reduced (Fig. 2D). A similar result of infiltrating leukocyte subsets was seen during the first attack on day 5 after tEAU induction (data not shown). These results suggest that S100A8/9 released by inflammatory cells might be associated with the recruitment of infiltrating cells, in particular, T cells and granulocytes.

**Paquinimod Treatment Significantly Inhibits R16-Specific T Cell Responses**

To further explore the role of the S100A8/9 complex in tEAU and the mechanism by which PA inhibits induction of tEAU, we measured R16-specific responses of T cells from the two groups of tEAU rats treated as in Figure 2A. As shown in Figure 3A, compared to control tEAU rats, PA-treated tEAU rats showed significantly decreased specific T cell proliferation not only on day 5 (left panel), but also on day 25 post-T cell transfer (right panel). This reduction was not due to cell death, since the day 25 PA-treated tEAU T cells contained similar numbers of apoptotic cells as control tEAU T cells when cultured in FCS-deficient medium for 24 hours (Fig. 3B) or 48 or 72 hours (data not shown).

Since both R16-specific Th1 and Th17 cells are pathogenic for tEAU induction, we examined whether PA treatment preferentially affected IFN-γ and/or IL-17<sup>+</sup> autoreactive T cells. As shown in Figure 3C, levels of IFN-γ (top panels) and IL-17 (bottom panels) released into the culture supernatants by T cells from PA-treated tEAU rats on both day 5 (left panels) and 25 (right panels) post-T cell transfer were markedly lower than those produced by T cells from control tEAU rats, indicating a long-lasting inhibitory effect of PA on pathogenic T cells (note treatment was stopped on day 10). In addition, antibody staining and flow cytometry of cells from day 25 (Fig. 3D) showed that 44.5% of T cells from control-treated tEAU rats expressed IFN-γ and 6.5% expressed IL-17, while the corresponding figures for PA-treated tEAU rats were 7.9% and 2.3%.

**R16-Specific T Cells Isolated From PA-Treated tEAU Rats Acquire Regulatory Activity**

In contrast, as shown in Figure 4A, R16-specific T cells from PA-treated tEAU rats on day 5 (left panels) or day 25 (right panel) produced significant higher amounts of IL-10 in response to antigenic challenge compared to cells from control tEAU rats. Examination of the phenotype of R16-specific T cells from PA-treated tEAU rats on day 25 showed that they expressed higher

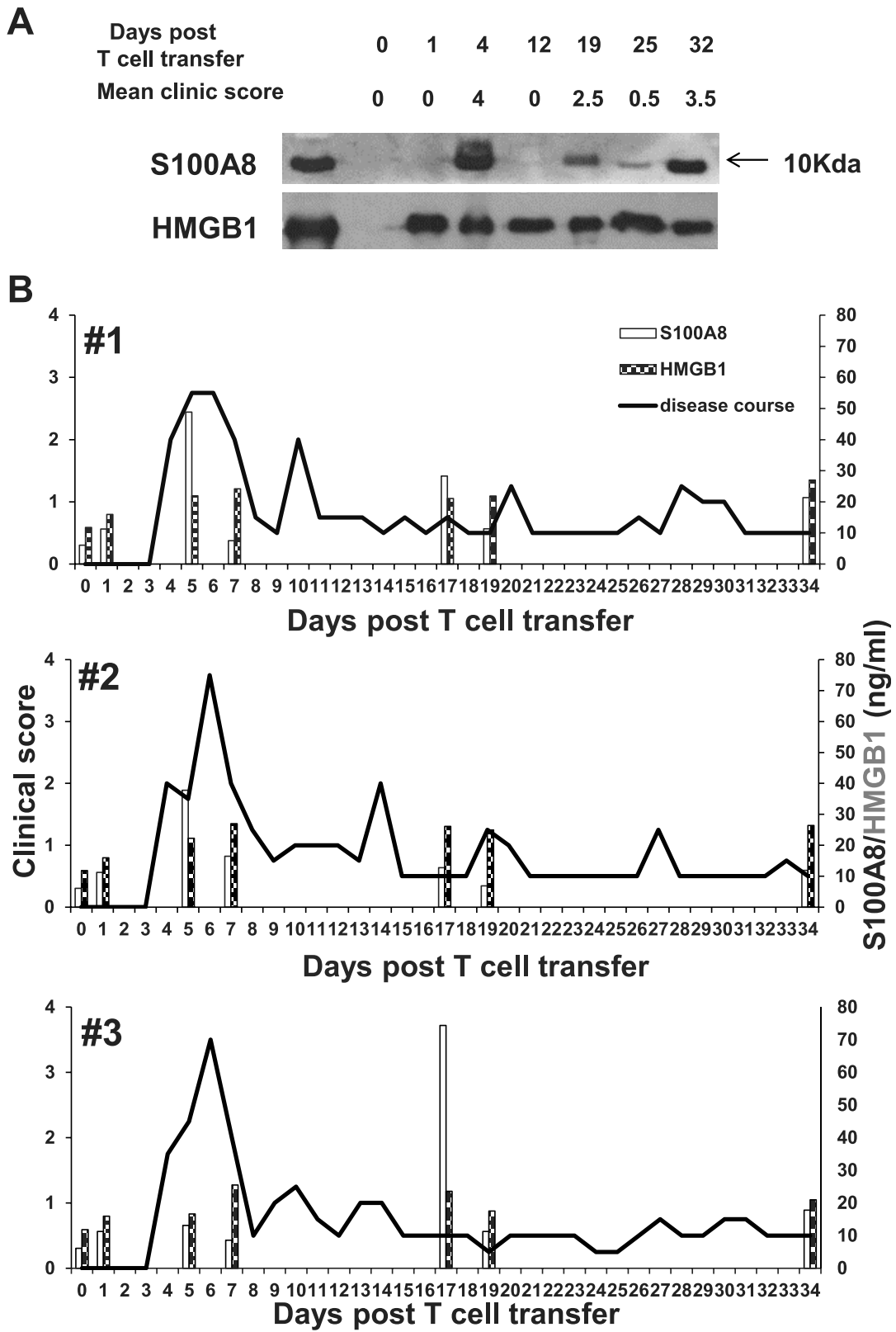


**FIGURE 1.** Changes in levels of extracellular S100A8 and HMGB1 in the eye and blood during the course of tEAU. (A) The clinical score of tEAU was noted and AqH samples collected on days 0, 1, 4, 12, 19, 25, and 32 posttransfer for S100A8 and HMGB1 levels determined by Western blotting. Lane 1 is the positive control (rat splenocytes). (B) tEAU was induced in three rats (#1–#3) and the clinical score recorded (indicated in red) and a blood sample taken at the indicated time point, then S100A8 and HMGB1 levels in the blood of each rat were determined by ELISA.

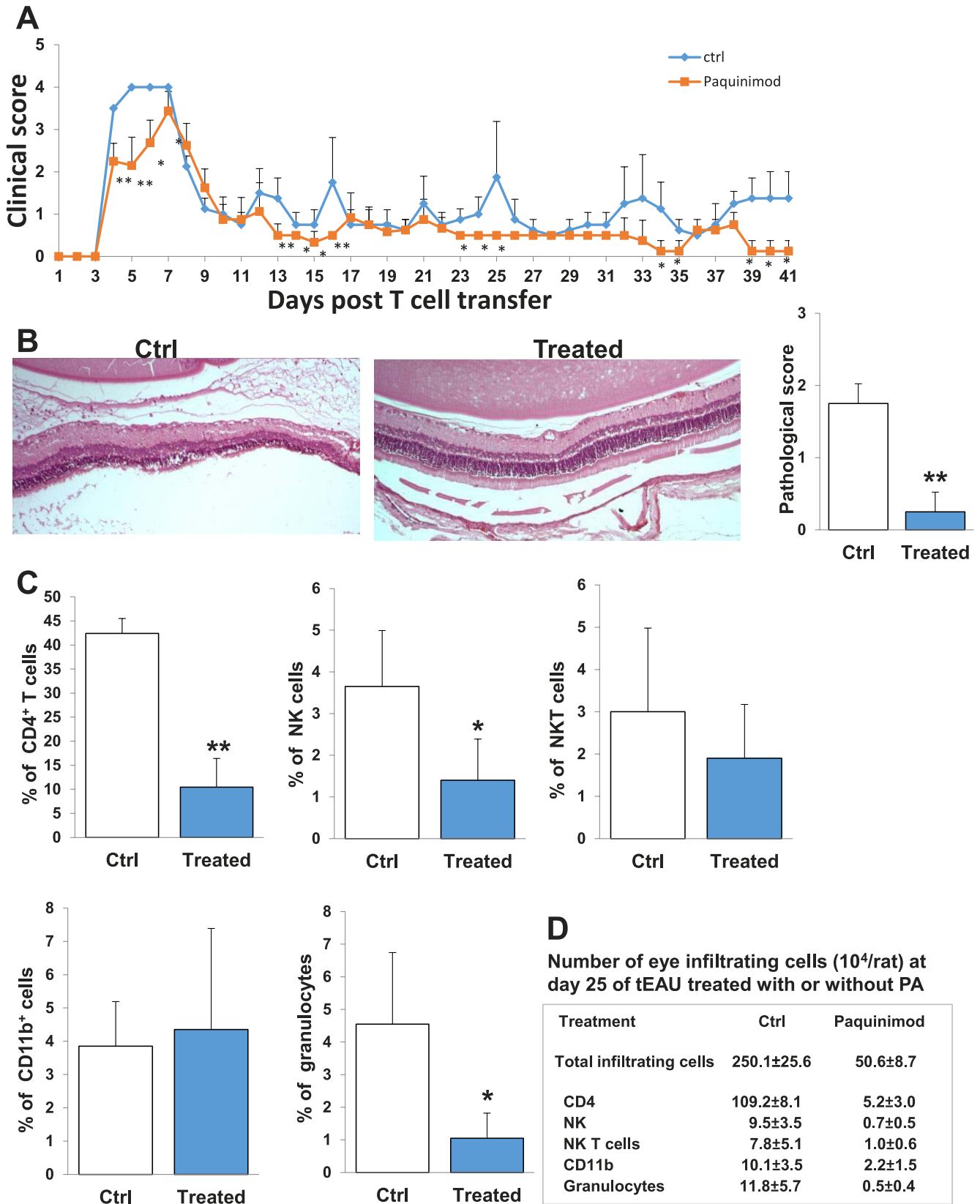


**FIGURE 2.** Disease evaluation after treatment with or without the S100A9 inhibitor paquinimod. Groups of rats were given with plain drinking water (Ctrl) or PA-containing drinking water as described in the Methods and Materials section and were used in the studies in Figures 2 to 6. (A) Disease severity was monitored daily by slit lamp microscopy for 41 days.  $n = 6-21$  animals per group.  $*P < 0.05$  and  $**P < 0.01$  compared to the Ctrl group using the Mann-Whitney  $U$  test. All values are expressed as mean  $\pm$  SEM. (B) Representative pathology for A on day 41 (left two panels). H&E; original magnification,  $\times 100$ , and mean  $\pm$  SD of pathological score from six rats on day 41 (right panel). (C) Percentage of different subsets of infiltrating leukocytes in the eye in the two groups examined by flow cytometry on day 25.  $n = 3$  rats in each group; all values are expressed as mean  $\pm$  SEM of two different experiments.  $*P < 0.05$  and  $**P < 0.01$  compared to the Ctrl group. (D) Summary of infiltrative cells, and subsets, from each rat of two different experiments is shown. Cells recovered from eyes of each group were counted after trypan blue staining. The number of cells was calculated based on the percentage of subsets as determined by flow cytometry.

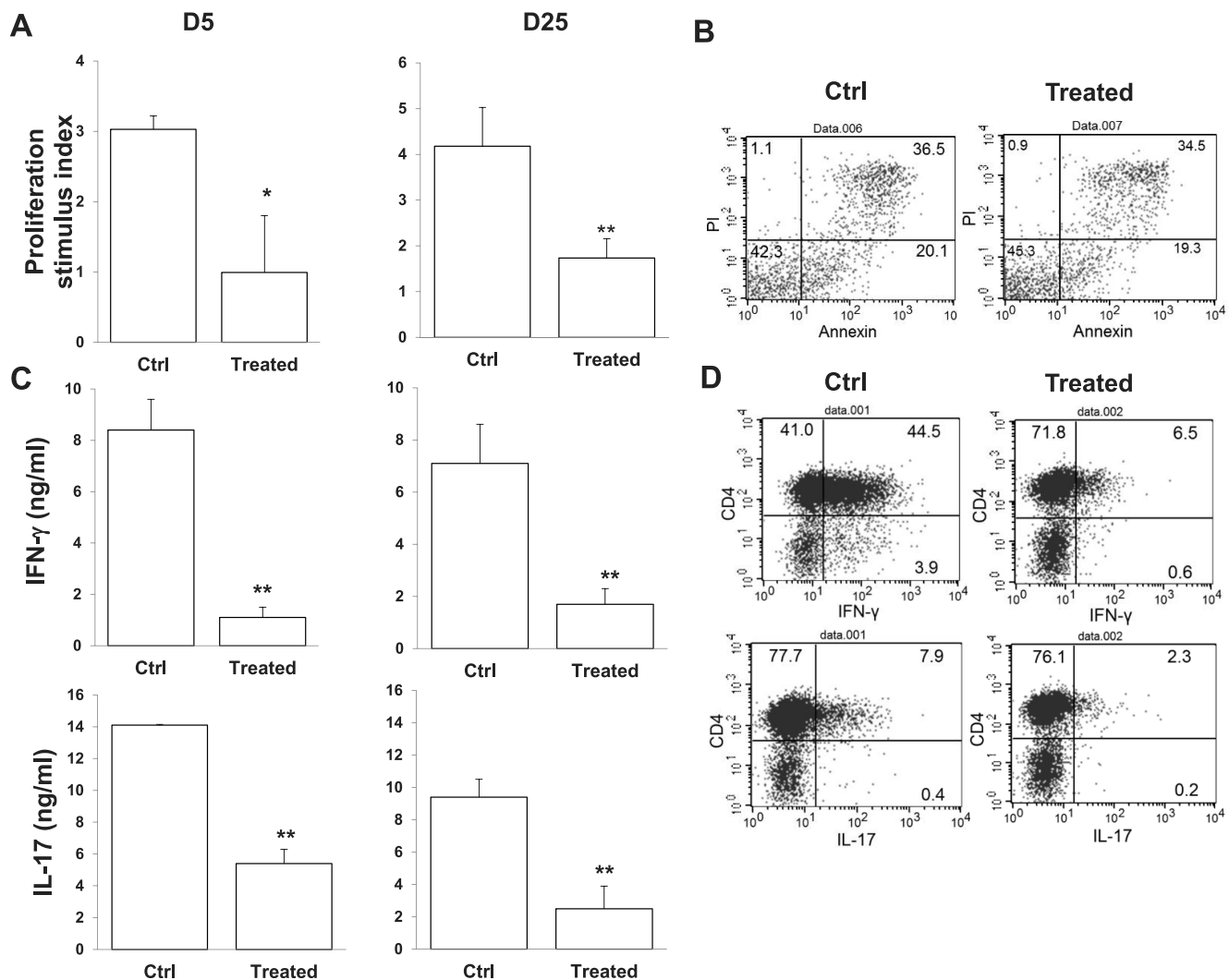


**FIGURE 3.** Low specific T cell responses in tEAU rats treated with paquinimod. Rats were treated as in Figure 2. (A) Responder T cells prepared on days 5 (*left panel*) and 25 (*right panel*) from the two groups of tEAU rats were incubated with 10 μg/mL R16 and their proliferation measured using the BrdU assay. Baseline data for T cells without antigen stimulation were 0.085 ± 0.012 (Ctrl) and 0.112 ± 0.034 (PA-treated) at D5, and 0.097 ± 0.02 (Ctrl) and 0.15 ± 0.06 (PA-treated) at day 25. (B) Responder T cells prepared on day 25 were cultured in FCS-free medium for 24 hours, then the fluorescence intensity of annexin V- and PI-gated T cells examined by flow cytometry. (C) Levels of IFN-γ (*top panels*) and IL-17 (*bottom panels*) released into the culture supernatants after 48-hour stimulation with R16 as described in (A) measured by ELISA. (D) At mean time, T cells were collected from C and frequencies of CD4<sup>+</sup>IFN-γ<sup>+</sup> and CD4<sup>+</sup>IL-17<sup>+</sup> T cells analyzed by flow cytometry. *n* = 3 rats in each group; representative of three separate experiments; all values are expressed as mean ± SEM. \**P* < 0.05 and \*\**P* < 0.01 compared to the Ctrl group. In (B) and (D), the percentage of positive cells is indicated on the gated cells.

levels of Foxp3 than responder T cells from control tEAU rats (Fig. 4B). In addition, we examined Tregs in the eyes of the control and treated groups and, as shown in Figure 4C, found that the percentage of Foxp3<sup>+</sup> T cells in the CD4<sup>+</sup> T cells was significantly increased in the eyes of PA-treated rats at both day 5 (*left panel*) and 25 (*right panel*). We then examined the *in vivo* disease-inducing ability of R16-specific T cells from PA-treated or control tEAU rats by injecting naïve Lewis rats with 5 × 10<sup>6</sup> R16-specific T cells isolated on day 16 from either PA-treated or control tEAU rats or with 5 × 10<sup>6</sup> cells from each group. As shown in Figure 4D, R16-specific T cells from control tEAU rats (*black line*) induced full disease upon transfer into naïve recipients, while those isolated from PA-treated tEAU rats (*blue line*) induced mild EAU without relapses. Moreover, T cells from PA-treated tEAU rats neutralized the pathogenic activity of R16-specific T cells isolated from control tEAU rats when both T cell populations were transferred into one rat (*red line*).

### The Effect of the S100A8/9 Inhibitor Is, in Part, on APCs

To examine whether the reduced proliferation of lymphocytes was a direct effect of the S100A8/9 inhibitor on T cells or an indirect effect on T cells via APCs, we performed crossover tests in which T cell proliferation was measured using all four combinations of responder T cells and APCs isolated on day 16 from the two sets of tEAU rats. As shown in Figure 5, T cells from PA-treated tEAU rats did not respond to increasing doses of R16 in the presence of APCs from either PA-treated or control tEAU rats, whereas T cells from control tEAU rats reacted well in the presence of APCs from control tEAU rats, but not PA-treated tEAU rats, indicating that dysfunction of both T cells and APCs contributed to the T cell hypo-responsiveness in PA-treated mice.

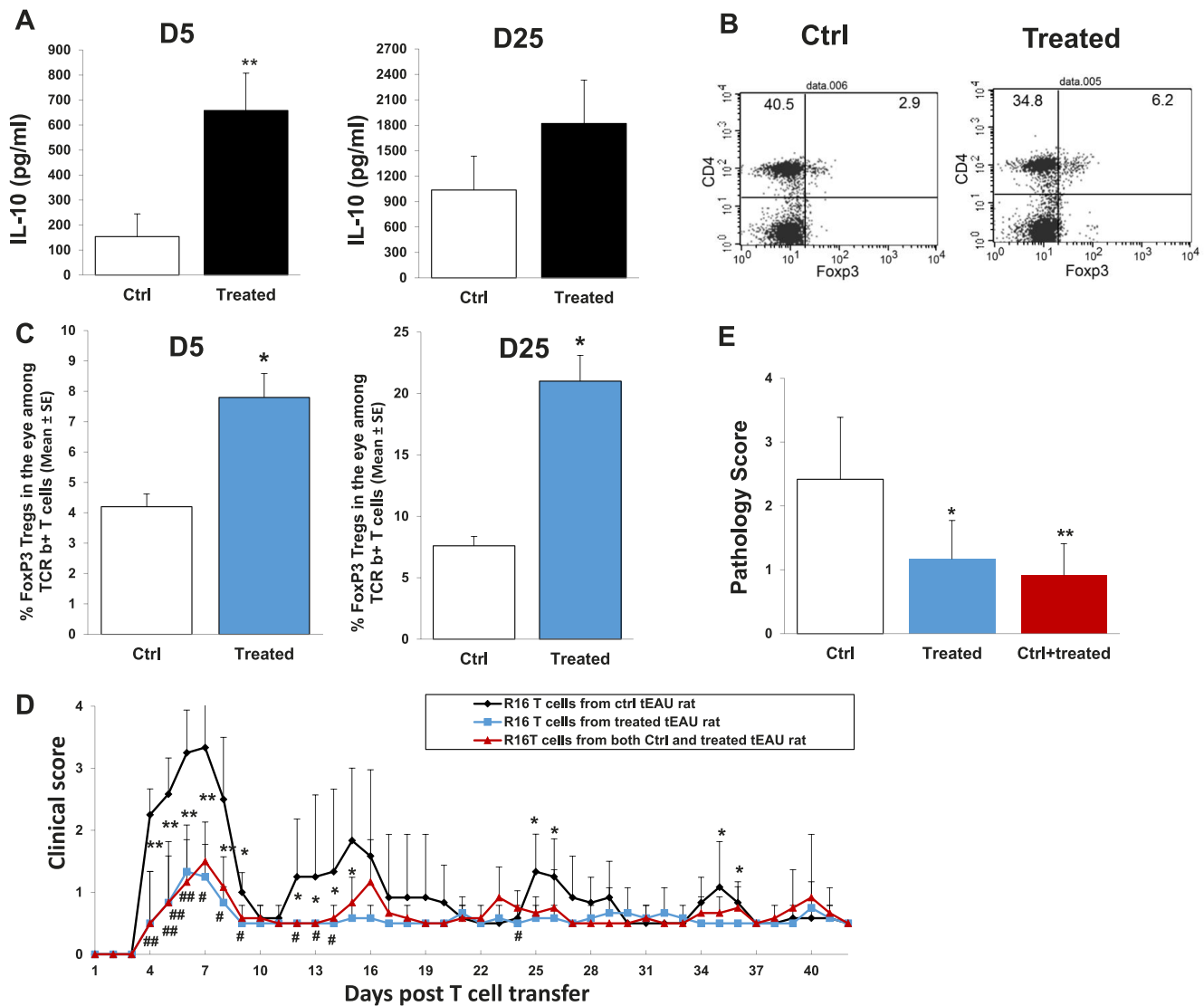


**FIGURE 4.** Paquinimod treatment enhances T regulatory cell activity. In (A) to (C), rats were treated as in Figure 2. (A, B) Responder T cells prepared on days 5 and 25 from the two groups of tEAU rats were stimulated as described in Figure 3A. IL-10 in the supernatants was assayed by ELISA (A) and percentage of CD4<sup>+</sup>FoxP3<sup>+</sup> cells among the stimulated T cells from day 25 of two groups analyzed by flow cytometry (B). (C) Percentage of FoxP3<sup>+</sup> cells among CD4<sup>+</sup>T cells in the eye in the two groups of tEAU rats on days 5 and 25 was examined by flow cytometry. A-D: *n* = 3 rats in each group; representative of three separate experiments; all values are expressed as mean ± SEM. \**P* < 0.05 and \*\**P* < 0.01 compared to the Ctrl group. (D) Recalled tEAU clinical scores (mean ± SEM) in three groups of naïve Lewis rats receiving stimulated R16-specific T cells from either PA- or control tEAU rats or both. *n* = 6 rats in each group; representative of two separate experiments. \**P* < 0.05 and \*\**P* < 0.01 are the clinical scores induced by R16 T cells from PA-treated tEAU rats compared to those induced by R16 T cells from Ctrl group; #*P* < 0.05 and ###*P* < 0.01 are the clinical scores induced by R16 T cells from both treated and ctrl tEAU rats compared to those induced by R16 T cells from Ctrl group. (E) Pathological scores (mean ± SEM) at the end of experiment D. \**P* < 0.05 and \*\**P* < 0.01 compared to the Ctrl group.

### PA-Treated APCs Show Reduced Expression of Costimulatory Molecules

To examine the phenotype of APCs from PA-treated tEAU rats, we looked at the expression of MHC class II and costimulatory molecules. As shown in Figure 6A, APCs isolated from PA-treated tEAU rats on day 16 expressed lower levels of MHC class II (difference not significant) and significantly lower levels of the costimulatory molecules CD86 and CD80 compared to the non-PA-treated tEAU rats, but significantly higher levels of CD200R.

We also examined the expression of MHC class II molecules and costimulatory molecules on APCs from tEAU that were incubated *in vitro* with 0, 1, or 5 μM S100A8 for 24 hours. As shown in Figure 6B, APCs exposed to S100A8 showed a dose-

dependent increase in levels of MHC molecules and CD80 and CD86 and a reduction in CD200R levels.

### DISCUSSION

There is extensive evidence that S100A8 is a very early and sensitive biomarker in experimental and clinical inflammation with various origins, such as infection, toxicity, trauma, cancer, and autoimmunity. Two decades ago, S100A8 was reported to be expressed by large ED1<sup>+</sup> monocytic perivascular cells that accumulate on days 11 to 14 of aEAU induced by immunization with a retinal antigen and complete adjuvant containing H37Ra mycobacterium tuberculosis (TB).<sup>29</sup> A recent article compared levels of S100A8/9 molecules in the AqH of Lewis rats in two



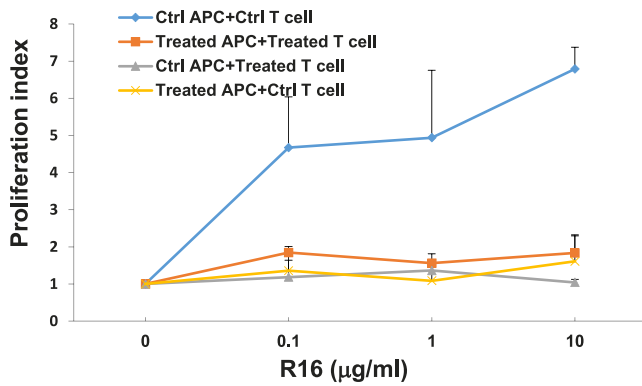


**FIGURE 5.** APCs from PA-treated rats lose the ability to activate T cells. Rats were treated as in Figure 2, then responder T cells and splenic APCs were prepared on day 16 from each group. Proliferation of all four combinations of T cells and APCs in the stimulation with increasing concentrations of R16 were measured. Baseline data for T cells without antigen stimulation were  $0.091 \pm 0.003$  (Ctrl APC and T cells),  $0.13 \pm 0.003$  (PA-treated APC and T cells),  $0.1 \pm 0.025$  (Ctrl APC and PA-treated T cells), and  $0.1 \pm 0.025$  (PA treated APC and Ctrl T cells). Representative of three separate experiments; all values are expressed as mean  $\pm$  SEM. \* $P < 0.05$  and \*\* $P < 0.01$  compared to the Ctrl group.

experimental inflammatory diseases, aEAU and primed mycobacterial uveitis (PMU; intraocular inflammation initiated by subcutaneous injection of TB H37Ra antigen followed by additional intravitreal injection of H37Ra) and found elevated S100A8 and S100A9 in both models of uveitis.<sup>30</sup> In the present study, we first demonstrated that local S100A8 levels correlated with recurrent episodes of autoimmune uveitis in a rat model induced by transfer of pathogenic effector T cells without the use of infectious macrobiotics that mimics the characteristics of human recurrent uveitis. Our results suggest that S100A8 might be a critical modulator in the initiation of recurrence and serve as a warning/danger signal for a flare of inflammation.

As shown in Figure 1A, S100A8 was not detected in the normal rat eye. The local increase in S100A8 might be due to a rapid influx of macrophages and other leukocytes, such as neutrophils, that express S100A8, and/or to activated tissue macrophages/microglia and dendritic cells. Since the inflammation only occurs in the eye, it is not surprising that, although systemic levels of S100A8/A9 were increased compared to the naïve control, serum levels did not correlate with uveitis activity. Our results are consistent with those in a recent clinical pilot study,<sup>31</sup> which showed (1) that, in idiopathic anterior uveitis (IAU) inflammation in the iris and ciliary body without systemic involvement, serum S100A8/9 levels were significantly higher than in healthy controls, but did not differ between IAU patients with active or inactive eye disease, whereas S100A8/A9 levels in the AqH of patients with IAU were higher than in nonuveitic controls, and (2) that, in juvenile idiopathic arthritis-associated uveitis, a form of uveitis

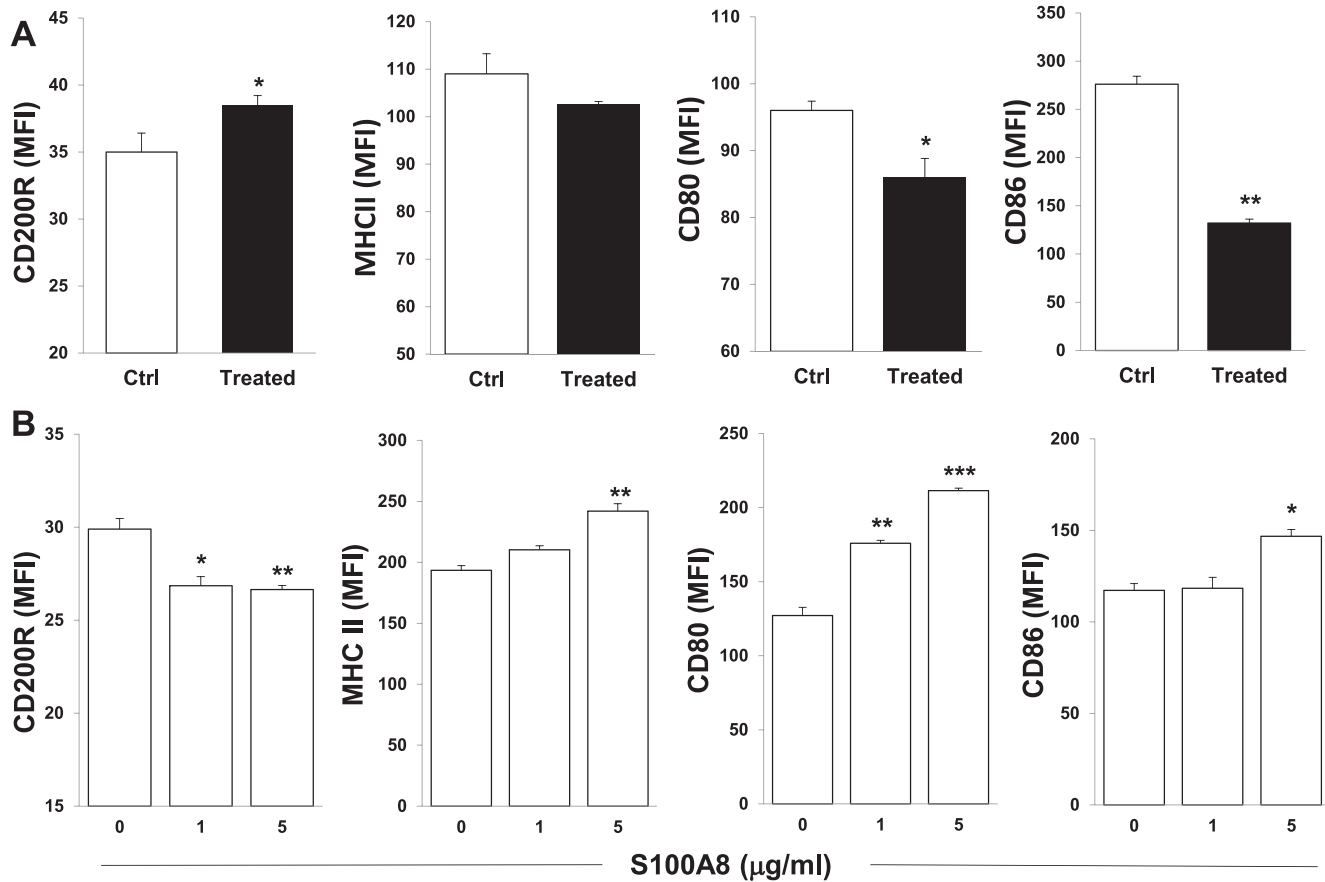


**FIGURE 6.** Expression of costimulatory molecules on APCs from PA-treated tEAU rats or in vitro treated with S100A8. Rats were treated as in Figure 2, then APCs isolated on day 16 were examined for expression of MHC class II and costimulatory molecules by flow cytometry analysis. (B) APCs isolated on day 16 from control treated tEAU rats were incubated in vitro with 0, 1, or 5 µM S100A8 for 24 hours, then were examined as above. Representative of three separate experiments; all values are expressed as mean  $\pm$  SEM. \* $P < 0.05$  and \*\* $P < 0.01$  compared to the Ctrl group.

with systemic involvement, S100A8/A9 levels were significantly elevated in both the AqH and serum compared to nonuveitis controls and the increase in serum S100A8/A9 levels correlated with uveitis activity.

Although extracellular S100A8/A9 levels are massively upregulated in diverse inflammatory autoimmune disorders,<sup>32,33</sup> little is known about their roles in adaptive immune responses and their effects on T and B cells. In 2010, Loser et al.<sup>22</sup> analyzed the effects of S100A8 and S100A9 in a mouse model of CD40L-induced dermatitis and showed that both are required for the development of functional autoreactive CD8<sup>+</sup> T cells. In their study, S100A8 and S100A9 induced IL-17 production in CD8<sup>+</sup> T cells in the animal model, and in vitro stimulation of CD8<sup>+</sup> T-cells from human subjects with active lupus erythematosus with S100A8 and S100A9 led to upregulation of IL-17 expression. A group of anti-inflammatory drugs, quinoline-3-carboxamides (Q compounds), has been demonstrated to specifically block the binding of S100A9 to TLR4 and RAGE.<sup>34</sup> Members of this drug family have shown proof-of-concept in clinical trials for the treatment of autoimmune diseases, such as multiple sclerosis,<sup>35</sup> systemic lupus erythematosus,<sup>26</sup> and Crohn's disease.<sup>36</sup> PA was found to reduce the priming of proinflammatory effector CD4<sup>+</sup> T cells in experimental autoimmune encephalitis<sup>25</sup> and selectively inhibit recruitment of Ly6C<sup>hi</sup> inflammatory monocytes and eosinophils during sterile peritoneal inflammation elicited by injecting necrotic tumor cells in B6 mice.<sup>37</sup> We therefore used PA to explore the role of the extracellular S100A8/A9 in adaptive immune responses and their effects on T cells in tEAU. Our data showed that oral administration of PA significantly protected rats from recurrences. The mechanisms by which PA reduced intraocular inflammation were (1) inhibition of recruitment of inflammatory cells into the eye (Fig. 2) and (2) a reduction in the numbers of R16-specific Th17 and Th1 cells and an increase in the numbers and functions of Tregs (Figs. 3, 4). Coinjection of PA-treated R16-specific T cells into naïve recipients prevented induction of tEAU by pathogenic R16-T cells, indicating an inhibitory function of Tregs. The results that the PA-treated T cells have inhibitory effects on T effector cells (Fig. 4) could be explained by increases in the number and function of Tregs, which might be in part converted from PA-treated T effector cells. By performing cross-proliferation tests in which T cell proliferation was measured using all combinations of responding T cells and APCs isolated from tEAU rats with or without treatment with PA, we found that increased Tregs in PA-treated tEAU rats might be due, in part, to an effect on APCs, which expressed reduced levels of CD80, CD86, and MHC class II antigen and increased levels of CD200R (Fig. 6A). CD200R functions as a coinhibitory receptor that, upon interaction with CD200, hinders myeloid cell function.<sup>38,39</sup> In addition, CD200 has also been demonstrated to downmodulate T and NK cell functions.<sup>40</sup> Whether increased expression of CD200R in APCs leads to reduced T effectors and increased Tregs requires further investigation. An opposite effect on the expression of these molecules was seen on APCs incubated in vitro with recombinant S100A8 (Fig. 6B). A previous study using PA in experimental autoimmune encephalomyelitis showed that PA ameliorates the disease by reducing effector T cell priming when given before disease induction by antigen immunization, and, on prolonged treatment, by selectively decreasing distinct subpopulations of splenic CD11b(+) myeloid cells.<sup>25</sup> Our results showing that PA treatment in tEAU increases Tregs, which might be in part converted from T effector cells demonstrates a new mechanism for the effect of PA in T cell-mediated autoimmune diseases.

In summary, our data show that the S100A8/A9 molecules play a critical role during recurrent uveitis, exerting and

amplifying autocrine and paracrine proinflammatory effects on APCs and T cells, and reducing numbers and function of Treg cells that promote inflammatory remission. In addition, S100A8 increases the expression of positive costimulatory molecules and reduces the expression of a negative costimulatory molecule. Our data demonstrate a link between local expression of DAMP molecules and autoimmune responses and suggest that complete S100A8/A9 blockade may be a new therapeutic target in recurrent uveitis.

### Acknowledgments

The authors thank the editorial assistance of Tom Barkas.

Supported in part by grant EY024051 from National Institutes of Health, Research to Prevent Blindness (RPB), the Commonwealth of Kentucky Research Challenge Trust Fund, and Kentucky Engineering and Science Foundation.

Disclosure: **J. Yun**, None; **T. Xiao**, None; **L. Zhou**, None; **R.W. Beuerman**, None; **J. Li**, None; **Y. Zhao**, None; **A. Hadayer**, None; **X. Zhang**, None; **D. Sun**, None; **H.J. Kaplan**, None; **H. Shao**, None

### References

- Suttorp-Schulten MS, Rothova A. The possible impact of uveitis in blindness: a literature survey. *Br J Ophthalmol*. 1996;80:844-848.
- Caspi RR. Immune mechanisms in uveitis. *Semin Immunopathol*. 1999;21:113-124.
- Shao H, Liao T, Ke Y, Shi H, Kaplan HJ, Sun D. Severe chronic experimental autoimmune uveitis (EAU) of the C57BL/6 mouse induced by adoptive transfer of IRBP1-20-specific T cells. *Exp Eye Res*. 2006;82:323-331.
- Shao H, Lei S, Sun SL, Kaplan HJ, Sun D. Conversion of monophasic to recurrent autoimmune disease by autoreactive T cell subsets. *J Immunol*. 2003;171:5624-5630.
- Shao H, Shi H, Kaplan HJ, Sun D. Chronic recurrent autoimmune uveitis with progressive photoreceptor damage induced in rats by transfer of IRBP-specific T cells. *J Neuroimmunol*. 2005;163:102-109.
- Deeg CA, Amann B, Raith AJ, Kaspers B. Inter- and intramolecular epitope spreading in equine recurrent uveitis. *Invest Ophthalmol Vis Sci*. 2006;47:652-656.
- Adamus G, Manczak M, Sugden B, Arendt A, Hargrave PA, Offner H. Epitope recognition and T cell receptors in recurrent autoimmune anterior uveitis in Lewis rats immunized with myelin basic protein. *J Neuroimmunol*. 2000;108:122-130.
- Ke Y, Jiang G, Sun D, Kaplan HJ, Shao H. Ocular regulatory T cells distinguish monophasic from recurrent autoimmune uveitis. *Invest Ophthalmol Vis Sci*. 2008;49:3999-4007.
- Jiang G, Ke Y, Sun D, Han G, Kaplan HJ, Shao H. Reactivation of uveitogenic T cells by retinal astrocytes derived from experimental autoimmune uveitis-prone B10RIII mice. *Invest Ophthalmol Vis Sci*. 2008;49:282-289.
- Jiang G, Sun D, Kaplan HJ, Shao H. Retinal astrocytes pretreated with NOD2 and TLR2 ligands activate uveitogenic T cells. *PLoS One*. 2012;7:e40510.
- Ke Y, Jiang G, Sun D, Kaplan HJ, Shao H. Retinal astrocytes respond to IL-17 differently than retinal pigment epithelial cells. *J Leukoc Biol*. 2009;86:1377-1384.
- Jiang G, Sun D, Yang H, Lu Q, Kaplan HJ, Shao H. HMGB1 is an early and critical mediator in an animal model of uveitis induced by IRBP-specific T cells. *J Leukoc Biol*. 2014;95:599-607.
- Yun J, Jiang G, Wang Y, et al. The HMGB1-CXCL12 complex promotes inflammatory cell infiltration in uveitogenic T cell-

- induced chronic experimental autoimmune uveitis. *Frontier Immunol.* 2017;8:142.
14. Jiang G, Wang Y, Yun J, et al. HMGB1 release triggered by the interaction of live retinal cells and uveitogenic T cells is Fas/FasL activation-dependent. *J Neuroinflammation* 2015;12:179.
  15. Kerkhoff C, Klempt M, Sorg C. Novel insights into structure and function of MRP8 (S100A8) and MRP14 (S100A9). *Biochimica et Biophysica Acta.* 1998;1448:200-211.
  16. Leach ST, Yang Z, Messina I, et al. Serum and mucosal S100 proteins, calprotectin (S100A8/S100A9) and S100A12, are elevated at diagnosis in children with inflammatory bowel disease. *Scand J Gastroenterol.* 2007;42:1321-1331.
  17. Foell D, Wittkowski H, Ren Z, et al. Phagocyte-specific S100 proteins are released from affected mucosa and promote immune responses during inflammatory bowel disease. *J Pathol.* 2008;216:183-192.
  18. van Lent PL, Blom AB, Schelbergen RF, et al. Active involvement of alarmins S100A8 and S100A9 in the regulation of synovial activation and joint destruction during mouse and human osteoarthritis. *Arthritis Rheum.* 2012;64:1466-1476.
  19. Schelbergen RF, Blom AB, van den Bosch MH, et al. Alarmins S100A8 and S100A9 elicit a catabolic effect in human osteoarthritic chondrocytes that is dependent on Toll-like receptor 4. *Arthritis Rheum.* 2012;64:1477-1487.
  20. Gebhardt C, Nemeth J, Angel P, Hess J. S100A8 and S100A9 in inflammation and cancer. *Biochem Pharmacol.* 2006;72:1622-1631.
  21. Sunahori K, Yamamura M, Yamana J, et al. The S100A8/A9 heterodimer amplifies proinflammatory cytokine production by macrophages via activation of nuclear factor kappa B and p38 mitogen-activated protein kinase in rheumatoid arthritis. *Arthritis Res Ther.* 2006;8:R69.
  22. Loser K, Vogl T, Voskort M, et al. The Toll-like receptor 4 ligands MRP8 and MRP14 are crucial in the development of autoreactive CD8+ T cells. *Nature Med.* 2010;16:713-717.
  23. van den Bosch MH, Blom AB, Schelbergen RF, et al. Alarmin S100A9 induces proinflammatory and catabolic effects predominantly in the M1 macrophages of human osteoarthritic synovium. *J Rheumatol.* 2016;43:1874-1884.
  24. Schelbergen RF, Geven EJ, van den Bosch MH, et al. Prophylactic treatment with S100A9 inhibitor paquinimod reduces pathology in experimental collagenase-induced osteoarthritis. *Ann Rheum Dis.* 2015;74:2254-2258.
  25. Helmersson S, Sundstedt A, Deronic A, Leanderson T, Ivars F. Amelioration of experimental autoimmune encephalomyelitis by the quinoline-3-carboxamide paquinimod: reduced priming of proinflammatory effector CD4(+) T cells. *Am J Pathol.* 2013;182:1671-1680.
  26. Bengtsson AA, Sturfelt G, Lood C, et al. Pharmacokinetics, tolerability, and preliminary efficacy of paquinimod (ABR-215757), a new quinoline-3-carboxamide derivative: studies in lupus-prone mice and a multicenter, randomized, double-blind, placebo-controlled, repeat-dose, dose-ranging study in patients with systemic lupus erythematosus. *Arthritis Rheum.* 2012;64:1579-1588.
  27. Liao T, Ke Y, Shao WH, et al. Blockade of the interaction of leukotriene b4 with its receptor prevents development of autoimmune uveitis. *Invest Ophthalmol Vis Sci.* 2006;47:1543-1549.
  28. Zhou L, Beuerman RW, Huang L, et al. Proteomic analysis of rabbit tear fluid: Defensin levels after an experimental corneal wound are correlated to wound closure. *Proteomics.* 2007;7:3194-3206.
  29. Deininger MH, Zhao Y, Schluesener HJ. CP-10, a chemotactic peptide, is expressed in lesions of experimental autoimmune encephalomyelitis, neuritis, uveitis and in C6 gliomas. *J Neuroimmunol.* 1999;93:156-163.
  30. Pepple KL, Rotkis L, Wilson L, Sandt A, Van Gelder RN. Comparative proteomic analysis of two uveitis models in Lewis rats. *Invest Ophthalmol Vis Sci.* 2015;56:8449-8456.
  31. Walscheid K, Heiligenhaus A, Holzinger D, et al. Elevated S100A8/A9 and S100A12 serum levels reflect intraocular inflammation in juvenile idiopathic arthritis-associated uveitis: results from a pilot study. *Invest Ophthalmol Vis Sci.* 2015;56:7653-7660.
  32. Foell D, Wittkowski H, Vogl T, Roth J. S100 proteins expressed in phagocytes: a novel group of damage-associated molecular pattern molecules. *J Leukocyte Biol.* 2007;81:28-37.
  33. Pruenster M, Vogl T, Roth J, Sperandio M. S100A8/A9: from basic science to clinical application. *Pharmacol Ther.* 2016;167:120-131.
  34. Bjork P, Bjork A, Vogl T, et al. Identification of human S100A9 as a novel target for treatment of autoimmune disease via binding to quinoline-3-carboxamides. *PLoS Biol.* 2009;7:e97.
  35. Comi G, Jeffery D, Kappos L, et al; ALLEGRO Study Group. Placebo-controlled trial of oral laquinimod for multiple sclerosis. *N Engl J Med.* 2012;366:1000-1009.
  36. D'Haens G, Lowenberg M, Samaan MA, et al. Safety and feasibility of using the second-generation pillcam colon capsule to assess active colonic Crohn's disease. *Clin Gastroenterol Hepatol.* 2015;13:1480-1486.
  37. Deronic A, Helmersson S, Leanderson T, Ivars F. The quinoline-3-carboxamide paquinimod (ABR-215757) reduces leukocyte recruitment during sterile inflammation: leukocyte- and context-specific effects. *Int Immunopharmacol.* 2014;18:290-297.
  38. Hoek RM, Ruuls SR, Murphy CA, et al. Down-regulation of the macrophage lineage through interaction with OX2 (CD200). *Science.* 2000;290:1768-1771.
  39. Wright GJ, Puklavec MJ, Willis AC, et al. Lymphoid/neuronal cell surface OX2 glycoprotein recognizes a novel receptor on macrophages implicated in the control of their function. *Immunity.* 2000;13:233-242.
  40. Farre D, Martinez-Vicente P, Engel P, Angulo A. Immunoglobulin superfamily members encoded by viruses and their multiple roles in immune evasion. *Eur J Immunology.* 2017;47:780-796.